https://doi.org/10.5194/amt-2019-420
Preprint. Discussion started: 5 February 2020

Atmospheric Measurement Techniques Discussions

Recommendations for Spectral Fitting of SO_2 from MAX-DOAS Measurements

Zoë Y. W. Davis[1] and Robert McLaren[2].

[1]Department of Earth and Space Science, York University, Toronto, M3J 1P3, Canada
[2]Department of Chemistry, York University, Toronto, M3J 1P3, Canada

Correspondence to: Zoë Davis (zoeywd@yorku.ca)

Abstract. Fitting SO_2 dSCDs from MAX-DOAS measurements of scattered sunlight is challenging because actinic light intensity is low in wavelength regions where the SO_2 absorption features are strongest. SO_2 dSCDs were fit with different wavelength windows (λ_{low} to λ_{high}) from ambient measurements with calibration cells of 2.2×10^{17} and 2.2×10^{16} molec cm^{-2} inserted in the light path at different viewing elevation angles. SO_2 dSCDs were the least accurate and fit errors were the largest for fitting windows with λ_{low} < 307 nm or λ_{low} >312 nm. The SO_2 dSCDs also exhibited an inverse relationship with the SO_2 absorption cross-section for fitting windows with λ_{low} < 307 nm. Spectra measured at low viewing elevation angles (i.e., $\alpha = 2^o$) exhibited less accurate SO_2 dSCDs for the same fitting windows compared to higher angles. The use of a 400 nm short-pass filter or a polynomial to account for stray light (the offset function), increased the accuracy of the SO_2 dSCDs for many different fitting windows, decreased fit errors, and decreased the dSCDs' dependence on the SO_2 absorption features. The inaccuracies at lower fitting wavelengths were increased by stray light originating from light with λ > 400 nm. Deviation of the SO_2 dSCD from the true value depended on the SO_2 concentration for some fitting windows rather than exhibiting a consistent bias. Uncertainties of the SO_2 dSCD reported by the fit algorithm were significantly less than the true error for many windows, particularly for the measurements without the filter or offset function. For retrievals with the filter or offset function, increasing λ_{high}> 320 nm tended to decrease the reported fit uncertainty but did not increase the accuracy. Based on the results of this study, a short-pass filter and a fitting window of 307.5 < λ <319 nm are recommended. If a filter is not available or conflicts with other species to be determined (NO_2, HCHO, etc.), the offset function should be enabled, and a fit window 307.5 < λ <319 nm is still recommended.

1 Introduction

The Differential Optical Absorption Spectroscopy (DOAS) technique has been used since its introduction by Brewer et al. (1973), Noxon (1975), Perner et al. (1976), and Platt et al. (1979) to measure atmospheric species with narrow-band structures of absorption in the visible and near UV wavelength region. A major challenge for the successful determination of trace-gas of Slant Column Densities (SCDs) using the DOAS method is the optimization of the retrieval parameters (Platt and Stutz, 2008; Vogel et al., 2013). These parameters depend on the atmospheric composition, measurement conditions, which DOAS instrument is used. The wavelength range of the retrieval ("fitting window") is a key parameter that depends

https://doi.org/10.5194/amt-2019-420
Preprint. Discussion started: 5 February 2020


Atmospheric Measurement Techniques Discussions

on the differential absorption features of the trace-gas (Vogel et al., 2013). Retrieval of differential SCDs (dSCDs) of SO_2 from Multi-Axis-DOAS (MAX-DOAS) measurements is challenging in a number of ways, including because the SO_2 absorption features are strongest in the wavelength region where the intensity of solar light becomes relatively small. There are three major regions of photo-absorption by SO_2 in the UV range: the very weak absorption in the A band from 340-390 nm, the moderately strong B band from 260-340 nm, and the strongest C band from 180-240 nm. MAX-DOAS spectroscopy uses the SO_2 "B band" in the near UV, which has absorption peaks of increasing strength with decreasing wavelength (Hermans et al., 2009; Xie et al., 2013). Actinic flux at the surface level of the earth decreases by several orders of magnitude in the 320-290 nm region due to a steep increase in O_3 absorption with decreasing wavelengths (Kreuter and Blumthaler, 2009). O_3 absorption features can also cause interference in the fit because of the similarity to the SO_2 absorption features between 315 and 325 nm (Rix et al., 2012). An additional challenge in the near UV region is that stray light in spectrometers reduces fit accuracy due to the low signal-to-noise ratio (Bobrowski et al., 2010; Kreuter and Blumthaler, 2009).

The optimal fitting window for SO_2 retrieval from MAX-DOAS spectra must have a lower wavelength (λ_{low}) small enough to include strong features of SO_2 absorption but large enough to ensure enough solar signal and prevent significant stray light effects. The upper wavelength of the fit range (λ_{high}) should ensure that the fitting window includes multiple SO_2 absorption structures while excluding wavelengths where SO_2 absorption features are so weak that degrees of freedom (DOF) are unnecessarily increased, increasing fitting uncertainty. An overly broad fit window also risks the inclusion of strong absorption features from other gases (Vogel et al., 2013) and increased errors due to insufficient correction of the broad-band terms (Marquard et al., 2000; Pukite et al., 2010). MAX-DOAS fit windows must be relatively narrow compared to direct sun viewing applications because the air mass factors used to convert SCDs to vertical column densities (VCD) differ with wavelength due to scattering (Fioletov et al., 2016). However, an overly narrow fit window can lead to cross-correlation between the reference absorption cross-sections (Vogel et al., 2013). Note that the optimal wavelength window may be present at higher wavelengths for measurements of very large column densities of SO_2 because the SO_2 optical densities in the B band can be >0.05, violating the DOAS assumption of weak absorption (Bobrowski and Platt, 2007; Fickel and Delgado Granados, 2017; Platt and Stutz, 2008). The absorptions of SO_2 become non-linear with wavelength at high concentrations in the typical fitting windows (<320 nm), which can lead to significant underestimation of the SO_2 column density (Bobrowski et al., 2010; Yang et al., 2007). Examination of SO_2 DOAS retrievals from OMI satellite measurements indicated reasonable results for the 310-365 nm range if column densities were <10 DU (2.69×10^{17} molec. cm^{-2}) but significant underestimation occurred for large column loadings (Yang et al., 2007). This effect is important for volcanic plume studies and in the most polluted urban and industrial environments.

Despite the importance of using an optimal fitting window, various windows have been used to retrieve MAX-DOAS SO_2 SCDs in the literature, and few studies attempted to assess the impact of the window's wavelength range on the SO_2 SCDs (Vogel et al., 2013). Fitting windows in previous MAX-DOAS studies include 305-317.5 nm (Tan et al., 2018), 307.5-328 (Schreier et al., 2015), 307.6-325 nm (Jin et al., 2016), 307.8-330 nm (Wang et al., 2017), 310-320 nm (Irie et al., 2011), and

https://doi.org/10.5194/amt-2019-420
Preprint. Discussion started: 5 February 2020

Atmospheric Measurement Techniques Discussions

307.5 to 315.0 nm (Bobrowski and Platt, 2007). Salerno et al. (2009) examined the sensitivity of SO_2 SCD to the fitting window in the 300-320 nm region using calibration cells of SO_2 of $3.2x10^{17}$ and $8.5x10^{17}$ molec. cm^{-2}. An optimal fitting window of 306.7-314.7 nm was determined based on the smallest SCD errors by varying the wavelengths of the fit window. However, the variations of the lower and upper window limits were only conducted for a single fixed upper limit and lower limit, respectively. Also, since the column densities were large, representative of volcanic plumes, the determined fitting window may non-ideal for smaller SO_2 column densities such as observed in urban studies. Fickel and Delgado Granados (2017) observed a high dependence of SO_2 SCDs from measurements of a volcano plume on the fitting window, particularly for large column densities. The authors suggested using different fitting windows for different column densities: 310-322 nm for SO_2 column densities $<10^{17}$ molec. cm^{-2}, 322-334 nm for column densities $>10^{18}$ molec. cm^{-2}, and 314.7-326.7 nm for intermediate column densities. A modelling study by Bobrowski et al. (2010) suggested using fitting windows in the higher 360-390 nm range for column densities on the order of 10^{19} molec. cm^{-2} because the SO_2 absorption features are much weaker. In this study, MAX-DOAS measurements of two different calibration gas cells with column densities of SO_2 representative of polluted urban conditions were conducted to examine the variation in the retrieved SO_2 dSCDs with 1) different fitting windows, 2) different viewing elevation angles (α), 3) the use of a 400 nm short-pass filter, and 4) the offset function enabled.

2 Methods

The mini-MAX-DOAS instrument (Hoffmann Messtechnik GmbH model #16127) consisted of a sealed metal box with a UV fibre-coupled spectrometer and all electronics inside. Incident scattered sunlight received by the cylindrical black telescope in front of the entrance optics is focused into the quartz fibre by a cylindrical quartz lens with a focal length of 40 mm. The spectrometer (OceanOptics USB2000 spectrograph) has a 50 µm wide entrance slit and a Sony ILX511 linear silicon Charge-Coupled Device (CCD) array detector (2048 pixels, pixel size 14x200 microns, signal-to-noise ratio at full signal 250:1). The spectral range of the spectrometer is 290-433 nm, with a resolution of ~0.6 nm FWHM. A Peltier stage cooled the spectrograph to maintain the chosen temperature of 5^{oC}. A stepper motor mounted underneath allows the instrument to point at different α above the horizon. The instrument was connected to a laptop via USB to transfer spectrometer data and allow automated measurements by Jscript programs using the DOASIS software package.

MAX-DOAS spectra of scattered solar light were recorded with an SO_2 calibration gas cell (Resonance Ltd.) inserted in the light path (in the telescope tube). The two cylindrical gas cells with a 22 mm diameter and 14.13 mm thickness had calibrated slant column densities (SCDs) of 2.2×10^{17} molec cm^{-2} (high) and 2.2×10^{16} (low) (+/- 10%) molec cm^{-2}. Active-DOAS measurements of the SO_2 gas cells confirmed the SCDs. These SCDs would be equivalent to an air mass with SO_2 mixing ratios of 87 and 9 ppb, respectively, for a $\alpha=30^o$ measurement within a homogeneous boundary layer of 1 km. For each cell, spectra were recorded around solar noon in September in Toronto, Ontario (43.773 N, -79.506 W) at $\alpha = 2^o$, 4^o, 8^o, 30^o, and 90^o above the horizon, followed by a 90^o measurement without the gas cell. This second zenith measurement was used as the Fraunhofer Reference Spectrum (FRS) in the fit. Each recorded spectrum was the average of 1000 spectra with

https://doi.org/10.5194/amt-2019-420
Preprint. Discussion started: 5 February 2020

Atmospheric Measurement Techniques Discussions

an integration time of ~115 ms. The experiment was repeated for both gas cells by placing a 400 nm short-pass filter (Edmund Optics TECHSPEC® OD 2 #47-285) within the telescope between the MAX-DOAS lens and the SO_2 gas cell. The fused silica filter had a thickness of 3 mm, a cut-off wavelength of 400 nm, and a transmission wavelength range of 250-385 nm. The blocking optical density was ≥2.0, and the transmission was >85% in the transmission range. Spectra collected using the filter were fit against a FRS collected by measuring a 90^o spectrum without a gas cell but including the filter.

Trace gas differential Slant Column Densities (dSCDs) were obtained using the DOAS (Platt and Stutz, 2008) with the DOASIS software (Institute of Environmental Physics, Heidelberg University, 2009). All spectra were corrected for dark current and electronic offset, and wavelength calibrated using measurements of a Mercury (Hg) lamp. Included in all fits were a Fraunhofer Reference Spectrum (FRS), Ring spectrum, a 3rd order polynomial, and cross-sections of SO_2 at 293K and O_3 at 293 and 223 K (Bogumil et al., 2003). The cross-sections were obtained from the MPI-MAINZ UV/VIS Spectral Atlas of Gaseous Molecules of Atmospheric Interest (Keller-Rudek et al., 2013). The reported uncertainty in the SO_2 absorption cross-section is ~3% (Bogumil et al., 2003). DOASIS fits dSCDs using an iterative algorithm based on the Levenberg-Marquardt method that finds the optimal solution by minimizing a cost function. The cost function includes the deviation between the measured spectrum and the spectrum modelled using the components included in the fit. Details on the DOASIS fitting algorithm can be found in Kraus (2006). The SO_2 dSCDs were fit in DOASIS with varying fitting windows using λ_{low}= 303-318 nm and λ_{high}= 310-340 nm in ~0.2 nm increments. The "retrieval interval mapping" technique (Vogel et al., 2013) was used to visualized and systematically evaluate the variations in the SO_2 dSCDs. The dSCDs are displayed as contour plots where λ_{low} and λ_{high} are the first and second dimensions, and the dSCDs are denoted using a colour scale.

For each calibration gas cell (high and low), four scenarios were fit: i) the base case (B) with no filter and no offset function, ii) no filter with offset function enabled (B+O), iii) with filter and offset disabled (B+F), and iv) with both filter and offset enabled (B+ F+O). SO_2 dSCDs were considered "accurate" if within ±10% of the high calibration cell value and ±50% of the low calibration cell value, 2.2×10^{17} and 2.2×10^{16} molec cm^{-2}, respectively. The background SO_2 in the atmosphere in Toronto was assumed to be negligible (<1 ppb) because there are currently no significant sources in Toronto (ECCC, 2018). A few industrial sources of <1600 tonnes of SO_2 yr^{-1} were present south-west of Toronto (ECCC, 2018), but the measurements were conducted under North-Easterly wind conditions. Typical hourly average mixing ratios of SO_2 in northern Toronto are <0.5 ppb (Ontario Ministry of the Environment, 2019).

3 Results

Examples of spectral retrievals of SO_2 from the α=2^o spectrum in the base case (no filter and offset function disabled) are shown in Fig. 1.

3.1 High Concentration Reference Cell

SO_2 dSCDs fit from the α=2^o and α=30^o measurements using the high concentration cell are shown in Fig. 2 with varying fitting windows for the four scenarios. The deviations of the SO_2 dSCDs from the expected value of 2.2×10^{17} molec cm^{-2} (fit errors) are shown in Fig. 3, where purple and green colours indicate under- and over-estimation, respectively. Grey and black

https://doi.org/10.5194/amt-2019-420
Preprint. Discussion started: 5 February 2020


Atmospheric Measurement Techniques Discussions

areas indicate that the dSCD under- and over-estimated the expected value by more than 8×10^{16} molec cm^{-2}, respectively. For the base case, the windows with λ_{low} <307 nm ("low wavelengths") underestimated the expected SO_2 dSCD, as indicated by the grey areas in Fig. 2 (B) and the purple areas in Fig. 3 (B). The addition of the short-pass filter increased the accuracy of the SO_2 dSCDs for most windows, especially in the low wavelengths (Figs. 2 & 3 (B+F)). These results suggest that stray light originating from wavelengths >400 nm increased the underestimation of SO_2 dSCDs at low wavelengths. Stray light is a well-known source of interference in spectroscopic measurements that reduces accuracy and can obscure weak spectral lines (Kristensson et al., 2014). Ideally, a spectrometer's detector receives only light with the correct spectral bandwidth window at each pixel (Lindon et al., 2000). Stray light is additional light of incorrect wavelength that enhances the background signal in ways that can vary across the spectral range (Kristensson et al., 2014). Sources of stray light include imperfections in the diffraction grating, leakage of light into the instrument, and scattering off mirrors and dust inside the instrument (Lindon et al., 2000). Stray light results in apparent negative deviations from Beer's law (Choudhury et al., 2015), causing an underestimation of the retrieved SO_2 dSCD by "filling-in" the measured intensity reduced by SO_2 absorption features and an underestimation of the real optical density (Bobrowski et al., 2010). Stray light has an enhanced effect at low wavelengths because of the low measured signal and sensitivity near the lower end of the actinic spectral range (Choudhury et al., 2015). Many fitting windows with λ_{low}<307 nm and λ_{high}< 320 nm still underestimated the SO_2 dSCD even with the filter (Fig. 2 (B+F)). This continued underestimation may be due to a combination of significant stray light from <400 nm and non-linearity effects due to large optical densities of SO_2 below 307 nm (>0.08) (Fig. 1) (see discussion in Section 1 and Bobrowski et al., 2010; Yang et al., 2007). Enabling the offset function increased the accuracy of the SO_2 dSCDs of many windows compared to the base case (Figs. 2 & 3 (B+O)). The offset function resulted in slightly more windows with accurate dSCDs than the filter for windows with λ_{low} <311 nm because the offset function attempts to compensate for all the stray light, not just the stray light originating from >400 nm (Fig. 2 (B+F) & (B+O)). The use of both the offset function and the filter slightly improved the dSCD accuracy for a few windows compared to the filter or offset function alone (Fig. 2 (B+F+O)). However, the effect for the lower angles was mostly for windows with large λ_{high} (>324 nm) that are unlikely to be utilized due to unnecessarily increased DOF.

Fitting windows produced more accurate SO_2 dSCDs from spectra measured at higher α (90^o & 30^o) compared to the lowest α (2^o & 4^o) in the base case (Figs. 2 & 3 (B) & S1). Windows with λ_{low} <307 nm underestimated SO_2 dSCDs more from the 2^o compared to the 30^o measurements (Fig. 3 (B)). The spectra collected at higher α are expected to produce more accurate SO_2 dSCDs because of the greater UV signal intensity (Fig. 4). Spectra measured at lower α have longer light paths closer to the ground, experiencing more Rayleigh scattering that preferentially scatters away shorter wavelengths and reduces the UV intensity. The impact of stray light on fits from the lower angle spectra is further increased because the visible light intensity, a potential source of stray light, is the same or higher compared to measurements at higher α (Fig. 4). The difference in the accuracy of SO_2 dSCDs between low and high α spectra decreased with the use of the filter or the offset function (Figs. 2-3), an expected result.

https://doi.org/10.5194/amt-2019-420
Preprint. Discussion started: 5 February 2020

Atmospheric Measurement Techniques Discussions

Fitting windows with λ_{low} >312 nm often overestimated the SO_2 dSCDs for all scenarios, as indicated by the green and black areas in Fig. 3, probably because the SO_2 absorption features become relatively weak (Fig. 4). Fickel and Delgado Granados (2017) proposed the use of the higher wavelength fitting window of 314.7-326.7 rather than 310-322 nm for SO_2 column densities between 10^{17} and 10^{18} molec. cm^{-2}. In contrast, the results of this study found that SO_2 dSCDs from the higher range were less accurate than the lower range. The threshold for using fitting windows with higher wavelengths due to large optical densities may be greater than 10^{17} molec. cm^{-2}.

The SO_2 dSCDs exhibited a dependence on the features of the SO_2 absorption cross-section for λ_{low} <307 nm for the base case (Figs. 2-3 (B)) that will be discussed in section 3.3.

3.2 Low Concentration Reference Cell

Figs. 5 and 6 show the SO_2 dSCDs and their deviations from the expected value (fit error), respectively, for the low concentration measurements for all the scenarios. Purple and green areas in Fig. 6 indicate dSCDs were under- and over-estimation, respectively. Black and grey areas indicate dSCDs over- and under-estimated by more than 2.0×10^{16} molec cm^{-2}, respectively. The SO_2 dSCDs from the base case exhibited a dependence on the SO_2 absorption that will be discussed in section 3.3. In the base case, the low concentration measurements had fewer windows that produced accurate SO_2 dSCDs compared to the high concentration measurements (Figs. 2 & 5 (B)). Most of the fitting windows produced SO_2 dSCDs that were >100% over- or under-estimated for the low concentration 2^o spectrum (Figs. 5 & 6 (B) & S1). In contrast, the low concentration 90^o measurement exhibited accurate SO_2 dSCDs for all fitting windows with λ_{low} < 311 nm (Fig. S1). This difference highlights that measurements at lower α experience greater inaccuracies from the reduced solar intensity and greater impact of stray light. While the high concentration dSCDs from the 2^o measurements were consistently underestimated for windows with λ_{low} <307 nm, the low concentration measurements often overestimated the dSCDs (Figs. 5 & 6 (B)). This overestimation in spite of the influence of stray light could be due to interference from O_3 since the similarity between the absorption features of SO_2 and O_3 can introduce instability in the retrieval (Kraus, 2006; Rix et al., 2012). The deviation of the dSCD from the true value can depend on the SO_2 concentration rather than exhibiting a consistent bias for a fitting window. The use of the filter or offset function increased the accuracy of the SO_2 dSCDs for most windows for spectra measured at angles ≤15^o (Fig. 3 & 6 (B+F), (B+O)). The improved accuracy due to the filter indicates that stray light originating from wavelengths >400 nm significantly decreased the accuracy of the SO_2 dSCDs for fitting windows at both lower and higher wavelengths. Unexpectedly, use of both the filter and offset function for the 30^o measurement reduced the accuracy of the SO_2 dSCDs compared to the base case for some windows with λ_{low}<307 nm and λ_{high}<320 nm (Fig. 6 (B+F+O)). Since the stray light to signal ratio is expected to be lower for the higher elevation measurements, and the filter already reduced the stray light, the offset function may have incorrectly estimated the relatively small amount of remaining stray light at some wavelengths. The offset function may have added unnecessary freedom to the fit, increasing instability and inaccuracy in the dSCD. Also, the offset function compensates for stray light by assuming the stray light is proportional to the measured intensity (see Eqs. 11-12 in Supplemental). If light from wavelengths outside the fitting window contributes to stray light, this assumption is invalid, and the offset function may increase uncertainty in the fit. The short-pass filter may

https://doi.org/10.5194/amt-2019-420
Preprint. Discussion started: 5 February 2020


Atmospheric Measurement Techniques Discussions

be the preferred method of reducing the impact of stray light compared to the offset function because the filter directly addresses rather than modelling the source of the problem. However, the problems from using both the filter and offset function can be mitigated by using a fitting window with λ_{low}<307 nm.

3.3 Dependence of the dSCD on the SO_2 Absorption Features

In the base case, the SO_2 dSCDs exhibited an inverse relationship with the SO_2 absorption features for windows with λ_{low}< 307 nm and λ_{high}<330 nm for non-zenith measurements (Figs. 2 & 5 (B)). The variation in the SO_2 dSCD as a function of λ_{low} from the $\alpha=2^o$ measurements, given λ_{high} of 315 nm and 324 nm, are shown in Figs. 7 and 8, respectively. The SO_2 dSCDs varied up to 3.4×10^{16} and 3.0×10^{16} molec cm^{-2} for a 0.4 nm change in λ_{low} for the high and low concentration measurements, respectively (Figs. 7-8). For both concentrations, using the filter or enabling the offset function reduced the dependence of the dSCDs on λ_{low} (Figs. 7-8) and increased the accuracy of many of the low wavelength fitting windows (Figs. 3 & 6). The SO_2 dSCD dependency was increased by stray light, exhibiting the greatest underestimation when λ_{low} coincided with an SO_2 absorption peak. Errors due to stray light are enhanced in wavelength regions where absorption is high (Choudhury et al., 2015). The measured signal was further reduced surrounding an SO_2 absorption peak (e.g., ~304.4 nm) compared to an absorption minimum and stay light "filled-in" the decreased intensity due to the absorption maxima. If an absorption peak is the strongest SO_2 feature included in the fit, the resultant deviation between the modelled and measured spectrum in the peak region requires the fit algorithm to underestimate the SO_2 dSCD to minimize the cost function (see Supplemental for fitting algorithm details). The inverse relationship between the dSCD and the SO_2 absorption features was strongest at λ_{low} <307 nm because absorption was greatest and solar signal was smallest (Figs. 4, 7 & 8). For the high concentration measurements, the dependence on the SO_2 features was likely enhanced by the increasing underestimation with decreasing wavelength due the increasing SO_2 optical depths included in the fit (absorption non-linearity effects). The dSCDs exhibited less dependence on the λ_{low} when λ_{low} = 307-311 nm due to increased solar intensity and weaker SO_2 absorption (Fig. 4). For both high and low concentration measurements, the anti-correlation of the SO_2 dSCD in the base case was more pronounced for windows with the λ_{high}= 324 nm than λ_{high}= 315 nm (Figs. 7-8).

3.4 Fit Uncertainties and Accuracy

The uncertainty in the SO_2 dSCD reported by the fitting algorithm and the actual deviation from the expected value shall be referred to as the "fit uncertainty" and the "fit error," respectively. The fit uncertainties from the 2^o spectrum are shown for the high and low concentration measurements in the left column of Figs. 9 and 10, respectively. The fit uncertainties for the base case were the greatest for windows with λ_{low} <306 nm and λ_{high} < 315 nm, and with λ_{low} >312 nm (Figs. 9 & 10 (B)). The differences between fit uncertainty and error are shown in the right columns of Figs. 9 and 10. The purple and black regions indicate that fit error was greater than the fit uncertainty, and the green regions indicate that fit error was less than fit uncertainty. For the high concentration measurement, the fit error was significantly greater than the fit uncertainty (by >2.2×10^{16} molec cm^{-2}) when λ_{low} <305 nm in the base case (black regions in Fig. 9 (B)). Therefore, fitting windows in low wavelength regions (impacted by stray light) not only produce less accurate SO_2 dSCDs but also significantly underestimate the fit error (Figs. 2, 3 & 9 (B)). For the low concentration measurement, the fit error was greater >1.1×10^{16} molec cm^{-2}

https://doi.org/10.5194/amt-2019-420
Preprint. Discussion started: 5 February 2020


Atmospheric Measurement Techniques Discussions

greater than the fit uncertainty for most windows in the base case (black regions in Fig. 10 (B)). The use of the filter or enabling the offset function reduced the fit uncertainties by up to 50% and decreased the difference between the fit errors and uncertainties, particularly for windows with λ_{low} <309 nm. Note that when the filter or offset function was used, increasing λ_{high} > ~ 320 nm or decreasing the λ_{low} < ~307 nm decreased the fit uncertainty but not the fit error for some windows (Figs. 6 & 8).

4 Summary & Recommendations

In the base case, SO_2 dSCDs were least accurate and had the largest fit uncertainties for fitting windows with λ_{low} <307 nm and >312 nm due to stray light and low solar signal, and weak SO_2 absorption, respectively. Fitting windows exhibited less accurate SO_2 dSCDs for spectra recorded at lower compared to higher α due to reduced UV signal. Therefore, choosing an accurate fitting window is particularly important for measurements at low α. Windows with λ_{low} <307 nm generally underestimated SO_2 dSCDs from high concentration measurements for all scenarios but could be overestimated by the same windows for the low concentration measurements. In the base, the SO_2 fit uncertainties were significantly less than the actual fit error for many windows for both concentration measurements. Using the short-pass filter or the offset function increased the accuracy of the SO_2 dSCDs, decreased fit uncertainty, and decreased the difference between the fit uncertainty and error compared to the base case for most windows. Some low wavelength windows continued to underestimate the SO_2 dSCDs despite the filter for the high concentration measurements, suggesting that significant stray light originated from <400 nm. A low pass filter with lower cut-off wavelength (i.e., $\lambda_{cut\text{-}off}$ = 340 nm) may aid in this respect, as may the use of spectrometers with reduced stray light. Non-linearity effects probably also contributed to under-estimation of the SO_2 dSCDs for λ_{low} <307 nm due to large optical depths of SO_2 at these wavelengths (e.g., >0.08). SO_2 dSCDs exhibited an inverse dependence on the features in the SO_2 absorption cross-section in the base case. The dependence decreased with the use of the short-pass filter or offset function, implying that stray light contributed to the dependence. Using both the filter and offset function decreased the accuracy of the low concentration dSCDs of SO_2 for some windows with λ_{low}<307 nm and λ_{high}<320 nm compared to the base case. Increasing the λ_{high} greater than ~ 320 nm tended to decrease the fit uncertainty but not necessarily the fit error for measurements with the filter or offset function.

Note that this study focused on the impact of two retrieval parameters (the fitting window wavelength and offset function) but that several other parameters can be varied in the SO_2 dSCD fit. These parameters include the order of the DOAS and offset function polynomials, and the choice of the literature cross-sections for the trace gases. Additional factors that could impact the retrieved dSCD include the solar zenith and azimuth angles during measurement. Future studies could repeat these experiments by measuring at different solar geometries and varying the other fit parameters. Also, SO_2 the column densities measured in this study were chosen to be representative of a range typical of polluted urban settings. For discussion of retrieving greater SO_2 column densities (>$1x10^{18}$ molec. cm^{-2}), see Bobrowski et al. (2010) and Fickel and Delgado Granados (2017).

Based on the results of this study, it is recommended that fitting windows for SO_2 have λ_{low} >307 nm to avoid the effects of stray light, low solar signal, and, for high column densities, non-linearity effects for optical densities >>0.05, and λ_{low} <312

https://doi.org/10.5194/amt-2019-420
Preprint. Discussion started: 5 February 2020


Atmospheric Measurement Techniques Discussions

nm because of weak SO_2 features. Fitting windows should have λ_{high} less than ~320 nm to avoid increased underestimation of the fit error. A fitting window should not be chosen because it has a smaller fit uncertainty since it does not guarantee a more accurate dSCD. A short-pass filter with a cut-off close to the λ_{high} of the SO_2 fitting window improves the accuracy of MAX-DOAS SO_2 measurements. In the absence of a filter or if a filter would conflict with other species to be determined (e.g., NO_2), the offset function should be used to compensate for stray light. Even in the case that SO_2 and NO_2 are to be fit simultaneously, a filter with $\lambda_{cut\text{-}off}$ = 550 nm may reduce stray light. A short-pass filter may be preferred over the offset function for reducing stray light impacts because the filter removes stray light while the offset function mathematically compensates for stray light by assuming it is proportional to the measured intensity (see Eqs. 11-12 in Supplemental). The offset function may increase fit error if this assumption is invalid or if little stray light is present. If a short-pass filter or the offset function is used, the 307.5-319 nm fitting window for SO_2 is recommended. Ultimately, the use of higher quality spectrometers with reduced stray light for MAX-DOAS measurements is desirable, but a higher expense.

Acknowledgements This research was funded by a Discovery Grant from the Natural Science and Engineering Research Council of Canada (NSERC) and a NSERC CREATE Grant- Integrating Atmospheric Chemistry and Physics from Earth to Space (IACPES).

https://doi.org/10.5194/amt-2019-420
Preprint. Discussion started: 5 February 2020

Atmospheric Measurement Techniques Discussions

Appendix A List of symbols and acronyms used in this paper.

Acronym	Expansion
α	Viewing Elevation Angle
$\lambda_{cut\text{-}off}$	Cutoff wavelength of Short-pass Filter
λ_{high}	Upper Limit Wavelength of Fitting Window
λ_{low}	Lower Limit Wavelength of Fitting Window
(B)	Base Case Measurement (No Filter and Offset Function Disabled)
(B+F)	Measurement with Short-Pass Filter
(B+F+O)	Measurement with Short-Pass Filter Fit using Offset Function
(B+O)	Measurement with Fit using Offset Function
dSCD	Differential Slant Column Density
FRS	Fraunhofer Reference Spectrum
HCHO	Formaldehyde
MAX-DOAS	Multi-Axis Differential Optical Absorption Spectroscopy
molec cm^{-2}	Molecules per square centimeter
nm	nanometers
NO_2	Nitrogen Dioxide
O_3	Ozone
ppb	Parts Per Billion
SCD	Slant Column Density
SO_2	Sulphur Dioxide
UV	Ultraviolet
VCD	Vertical Column Density

https://doi.org/10.5194/amt-2019-420
Preprint. Discussion started: 5 February 2020

Atmospheric Measurement Techniques Discussions

Figs. & Tables

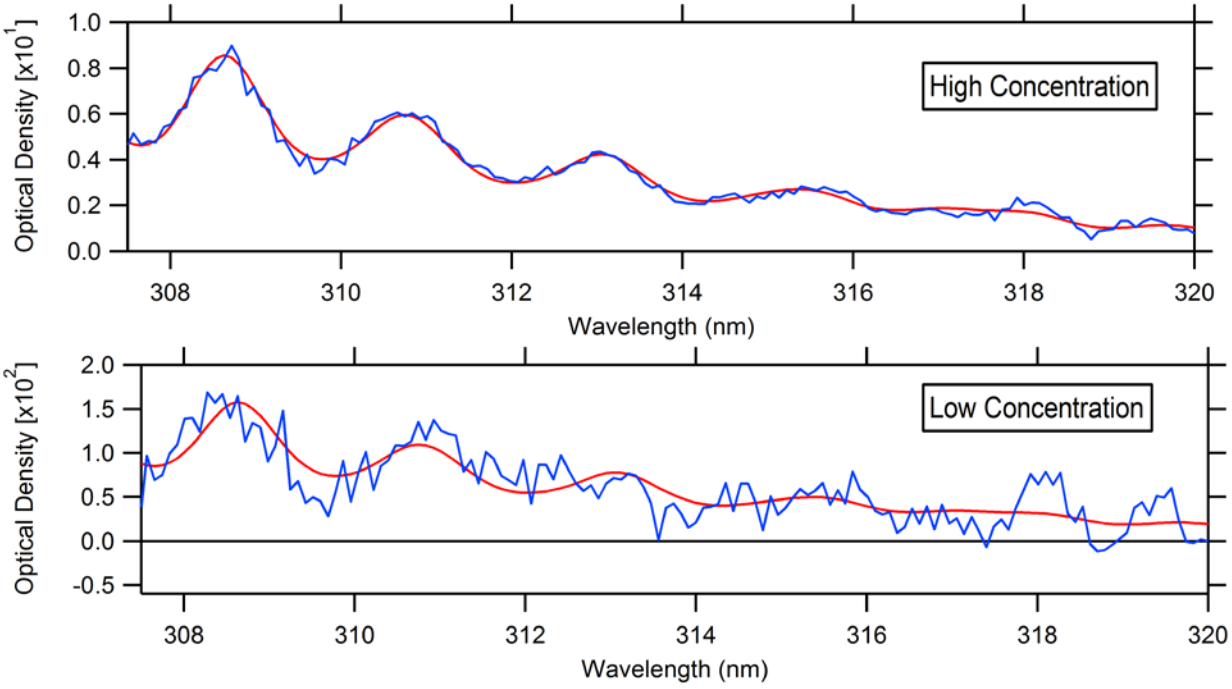

Figure 1 Examples of spectral retrievals of SO_2 from the base case (no filter and offset function disabled) from spectra measured at 2° viewing elevation angle using the fitting window 307.5-320 nm. Retrieved dSCDs were 2.23(+/-0.08)×10^{17} molec cm^{-2} and 4.10(+/-0.66)×10^{16} molec cm^{-2} for the high and low concentration measurements, respectively.

https://doi.org/10.5194/amt-2019-420
Preprint. Discussion started: 5 February 2020

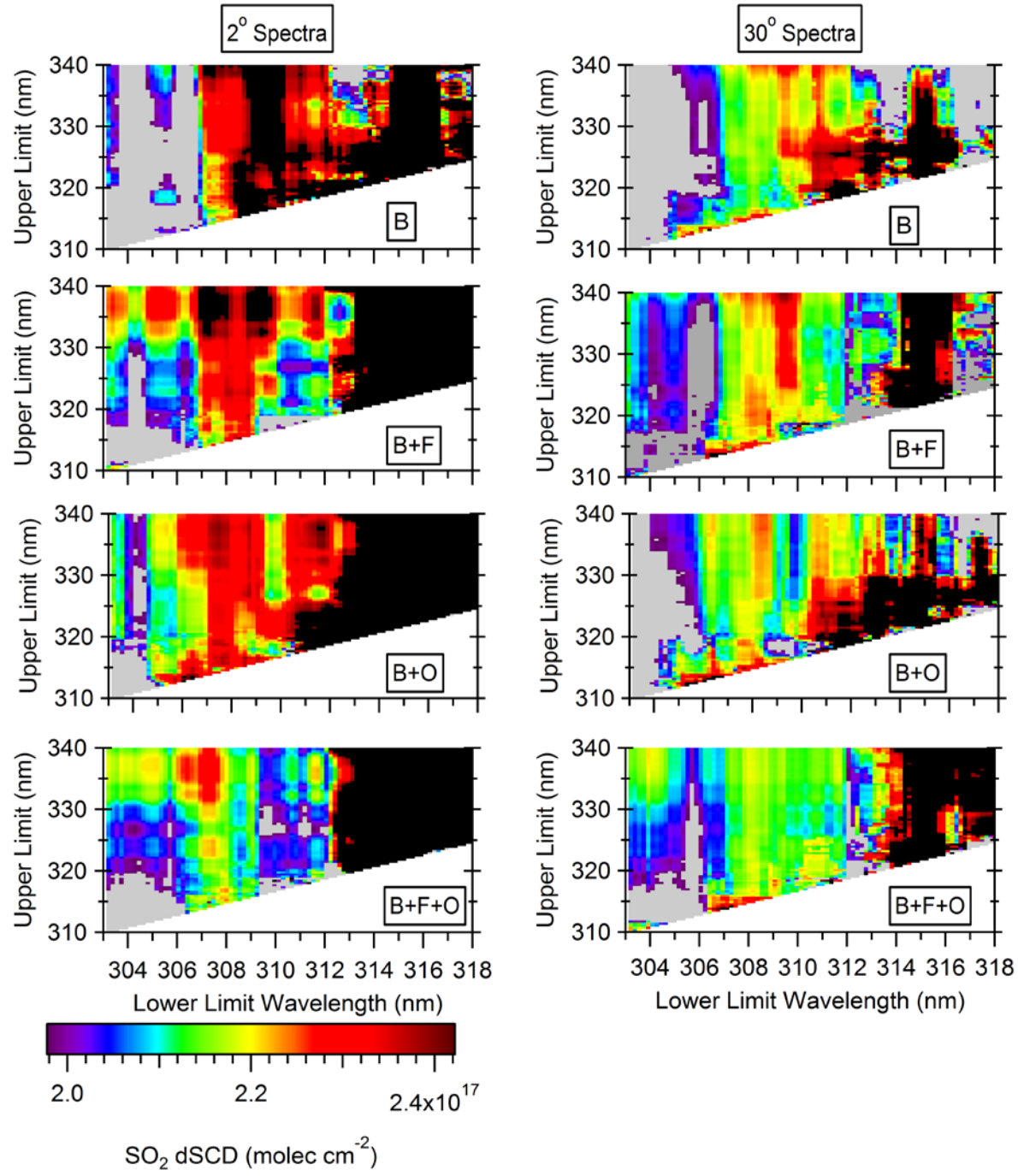

Figure 2 SO_2 dSCDs fit from high concentration measurements at 2° (left) and 30° (right) elevation angles for the base case (B), with offset (B+O), with filter (B+F), and with filter and offset (B+F+O). Grey and black areas indicate dSCDs were <10% less and >10% more than the expected value, respectively. The true value of the cell is 2.2×10^{17} molec cm^{-2} (yellow).

https://doi.org/10.5194/amt-2019-420
Preprint. Discussion started: 5 February 2020

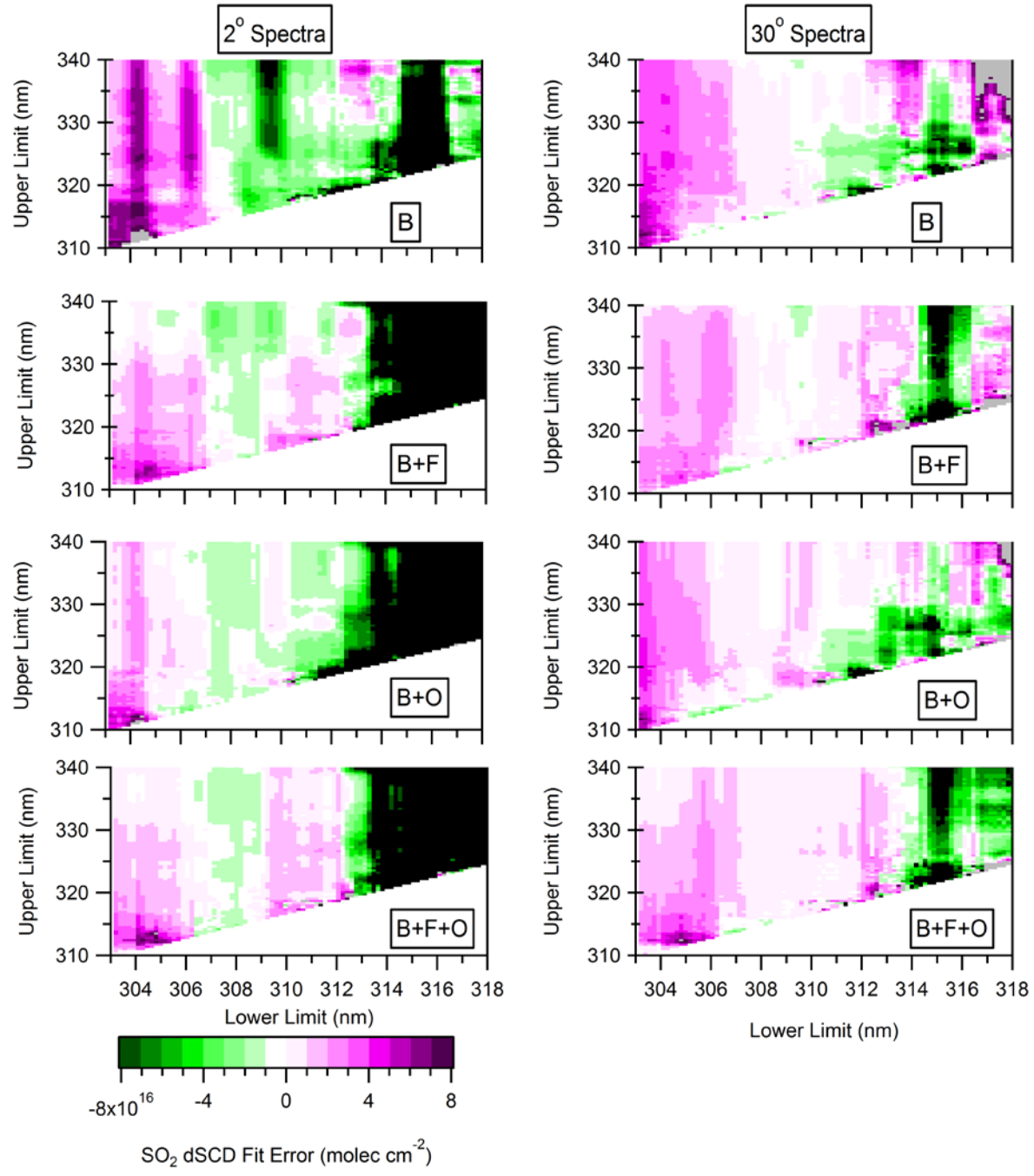

Figure 3 High concentration fit errors (deviations of SO_2 dSCDs from the expected value of 2.2×10^{17} molec cm^{-2}) from the measurements at 2^o (left) and 30^o (right) elevation angles for the base case (B), with offset (B+O), with filter (B+F), and with filter and offset (B+F+O). Purple and green areas indicate under- and over-estimation of the expected value, respectively. Black and grey areas indicate dSCDs over- and under-estimated by more than 8.0×10^{16} molec cm^{-2}, respectively.

https://doi.org/10.5194/amt-2019-420
Preprint. Discussion started: 5 February 2020

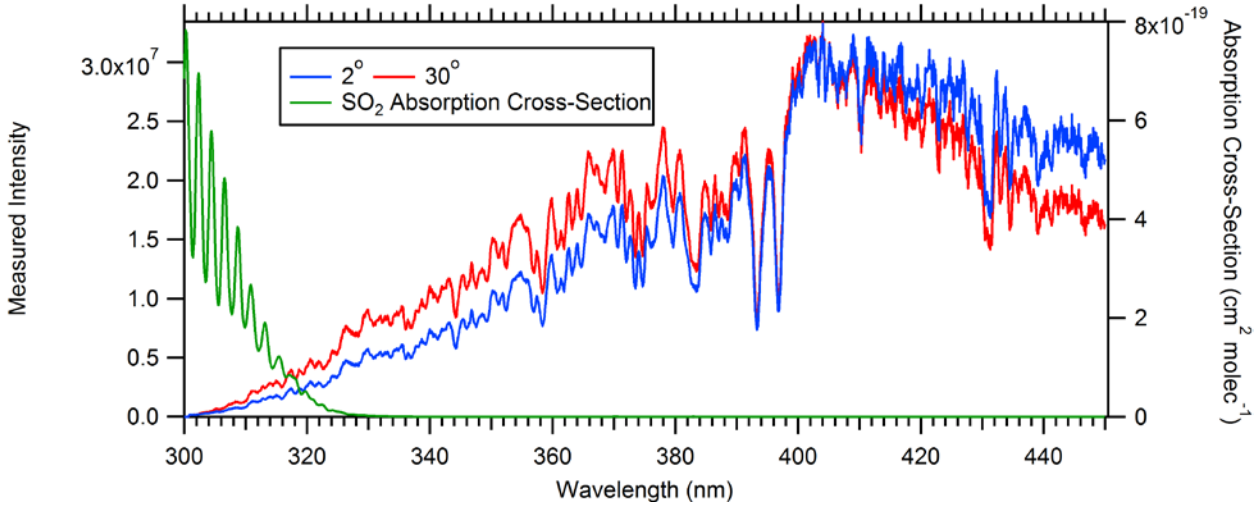

Figure 4 Comparison of the measured spectral intensity for the 2° and 30° viewing elevation angle spectra with the low concentration cell without the short-pass filter, and the absorption cross-section of SO_2 smoothed to the spectral resolution of the instrument.

https://doi.org/10.5194/amt-2019-420
Preprint. Discussion started: 5 February 2020

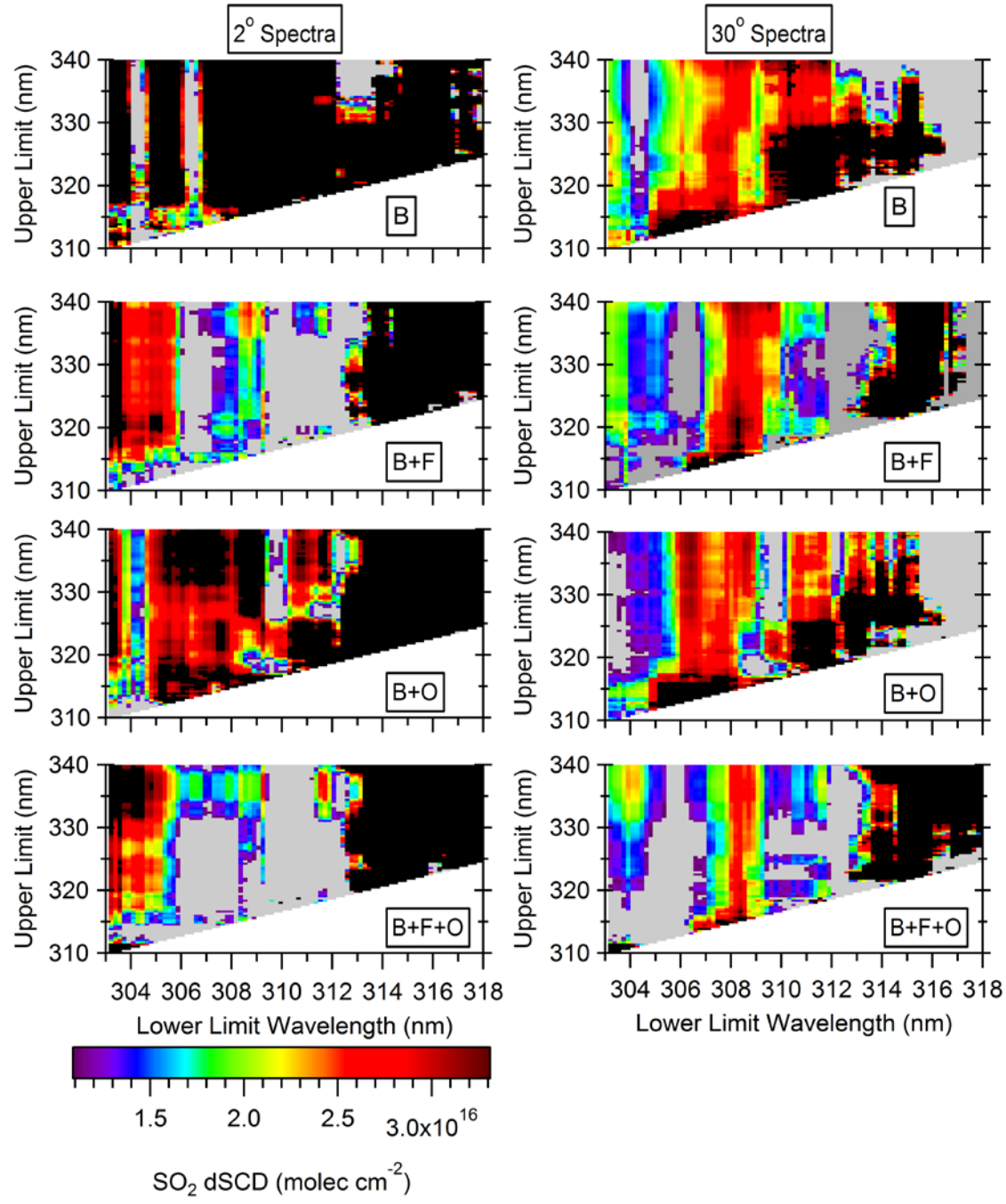

Figure 5 SO_2 dSCDs fit from the low concentration measurements at 2° (left) and 30° (right) elevation angles for the base case (B), with offset (B+O), with filter (B+F), and with filter and offset (B+F+O). Grey and black areas indicate dSCDs that were <50% less and >50% more than the expected value, respectively. The true value of the high concentration cell is 2.2×10^{16} molec cm^{-2} (yellow).

https://doi.org/10.5194/amt-2019-420
Preprint. Discussion started: 5 February 2020

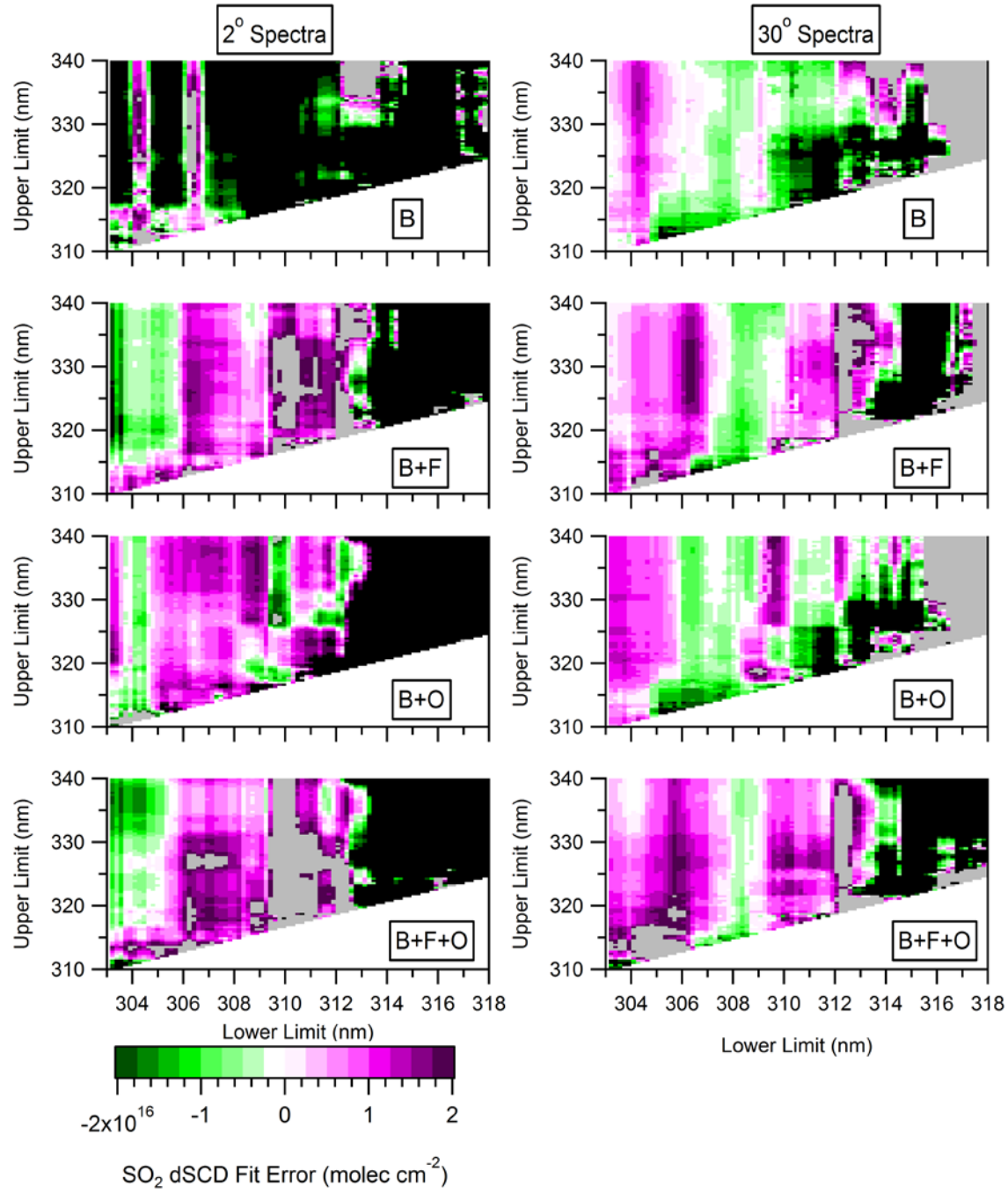

Figure 6 Low concentration fit errors (deviations of SO_2 dSCDs from the expected value of 2.2×10^{16} molec cm^{-2}) from the measurements at 2° (left) and 30° (right) elevation angles for the base case (B), with offset (B+O), with filter (B+F), and with filter and offset (B+F+O). Purple and green areas indicate dSCDs were under- and over-estimation, respectively. Black and grey areas indicate dSCDs over- and under-estimated by more than 2.0×10^{16} molec cm^{-2}, respectively.

https://doi.org/10.5194/amt-2019-420
Preprint. Discussion started: 5 February 2020

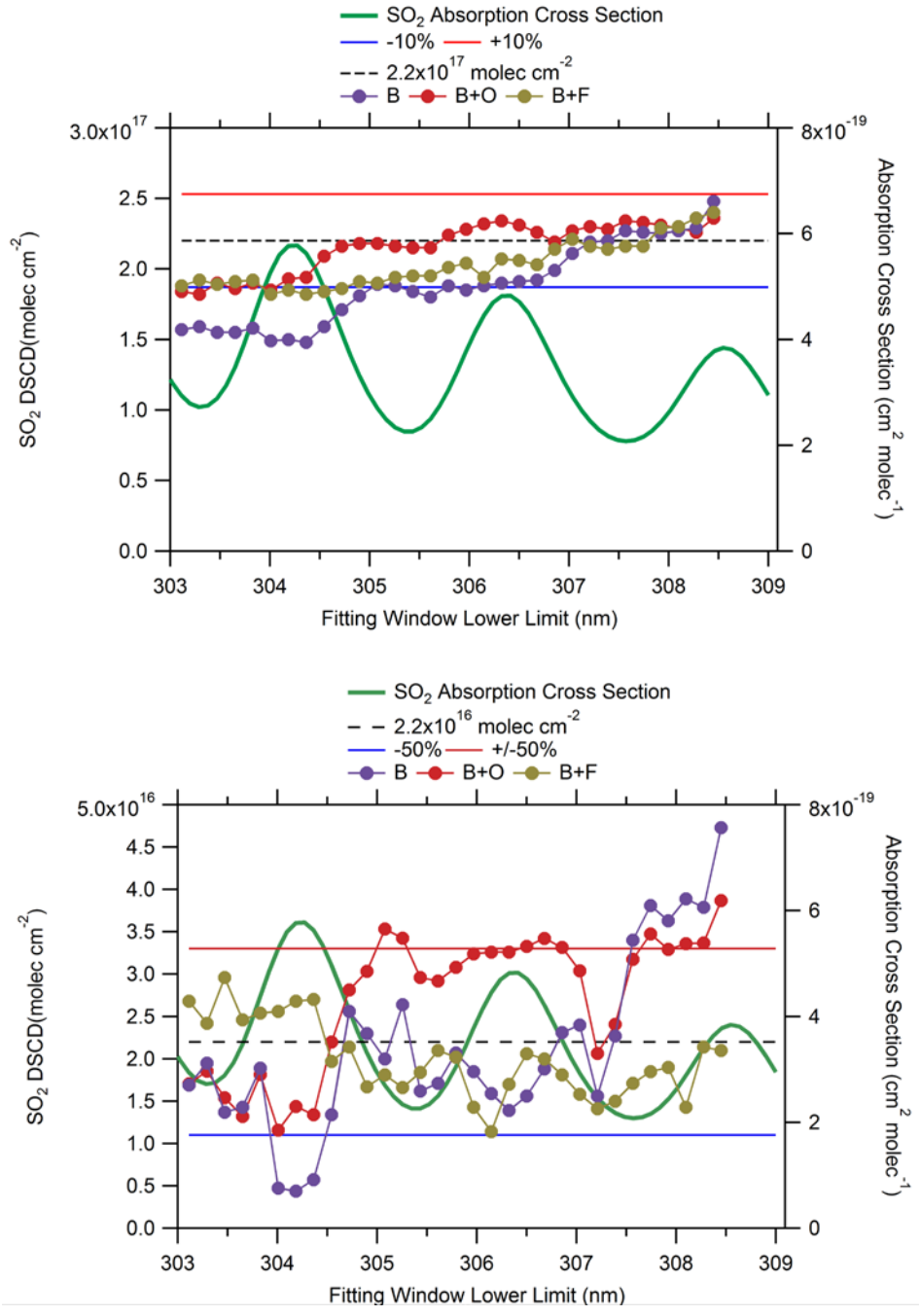

Figure 7 SO_2 absorption cross-section and variation in the SO_2 dSCD with λ_{low} with λ_{high} = 315 nm for high (top) and low (bottom) concentration measurements for the base case (B), with offset (B+O), and with filter (B+F).

https://doi.org/10.5194/amt-2019-420
Preprint. Discussion started: 5 February 2020

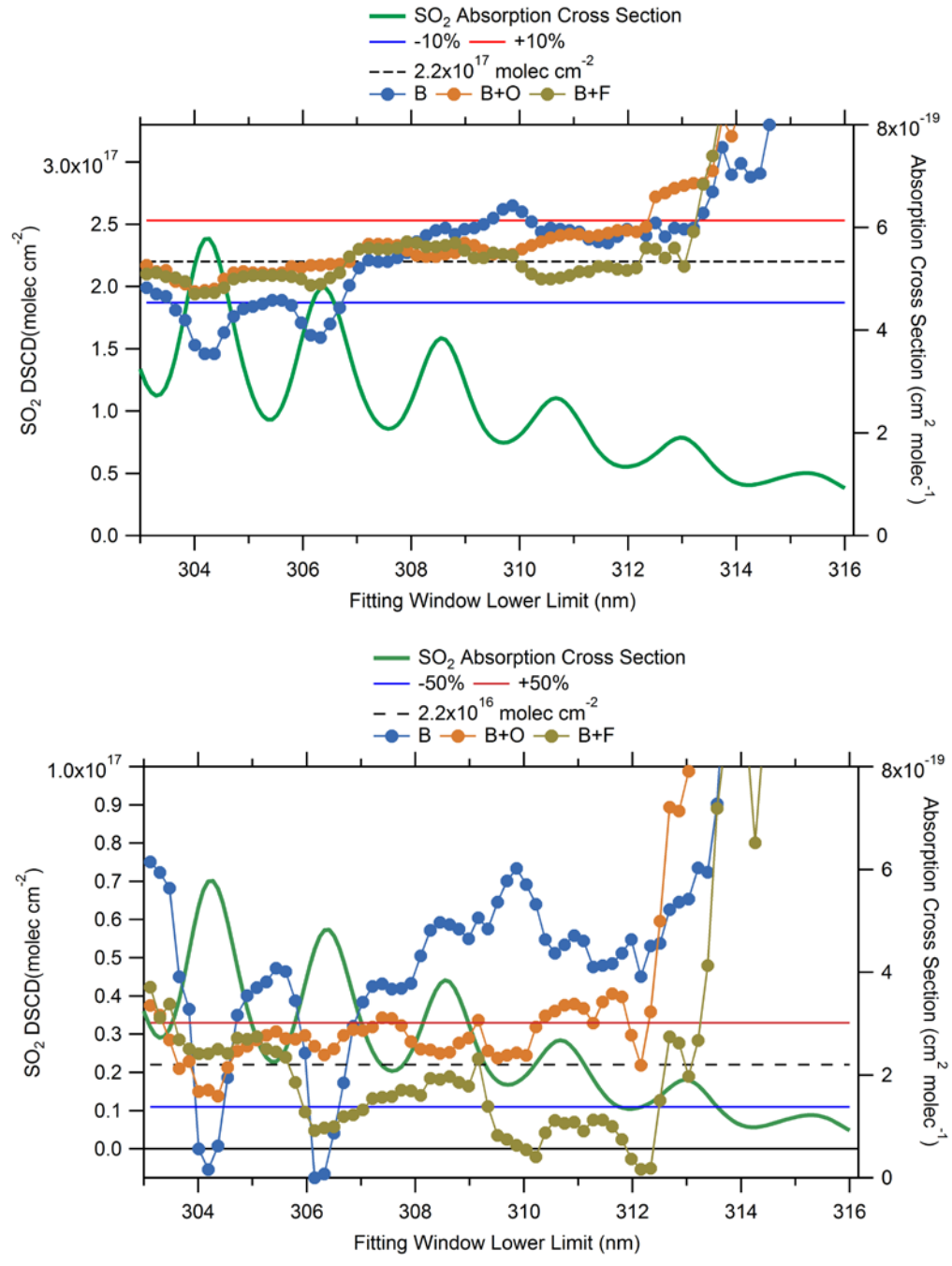

Figure 8 SO_2 absorption cross-section and variation in the SO_2 dSCD with λ_{low} with λ_{high}= 324 nm for high (top) and low (bottom) concentration measurements for the base case (B), with offset (B+O), and with filter (B+F).

https://doi.org/10.5194/amt-2019-420
Preprint. Discussion started: 5 February 2020

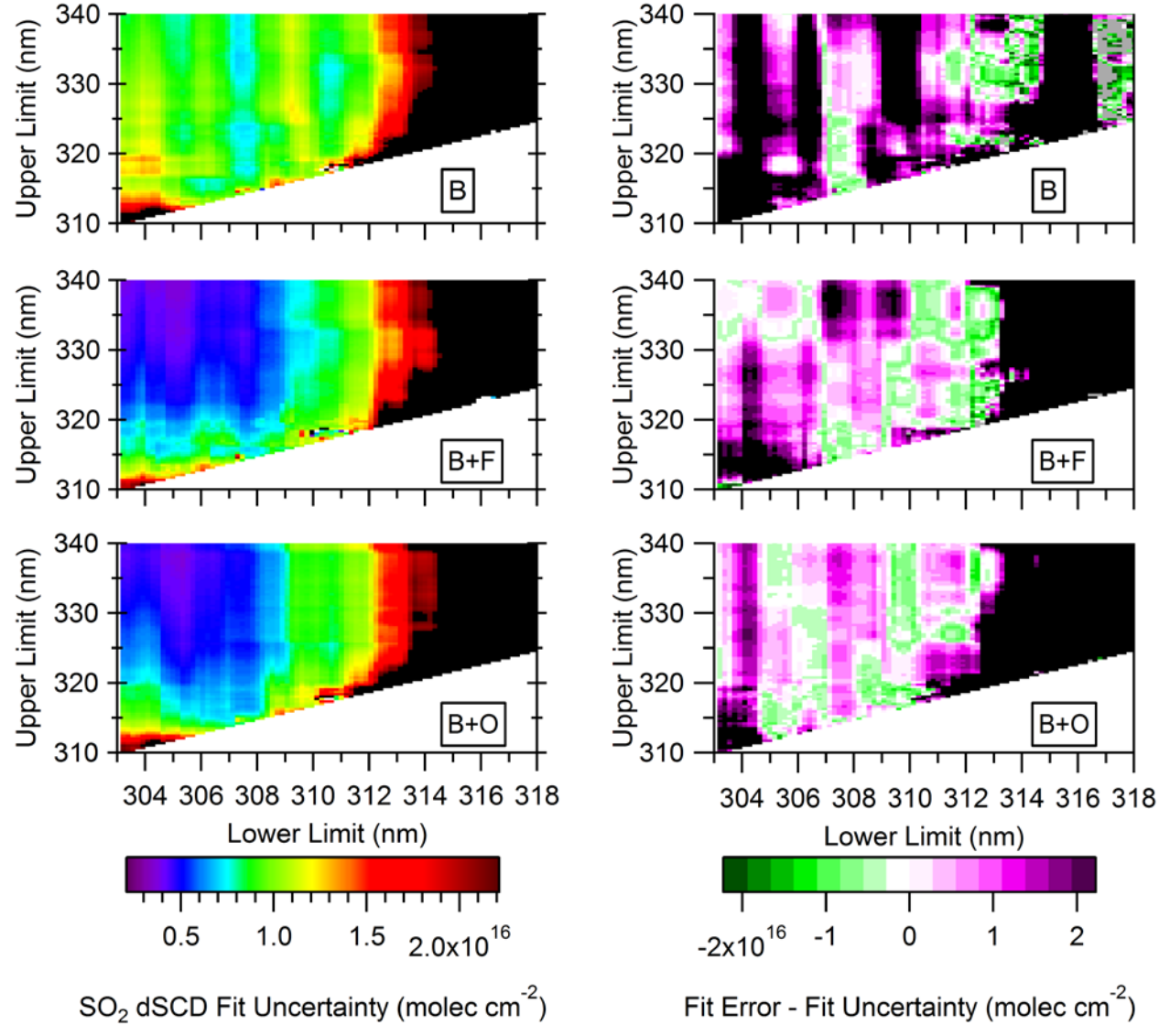

Figure 9 High concentration SO_2 dSCDs fit uncertainties (left) and difference between fit error and uncertainty (right) from spectra measured at 2^o elevation angle for the base case (B), with offset (B+O), and with filter (B+F). Black areas indicate errors $>1.1\times10^{16}$ molec cm^{-2} for absolute error (left) and $>2.2\times10^{16}$ molec cm^{-2} for the difference (under-estimation) between actual and fit error.

https://doi.org/10.5194/amt-2019-420
Preprint. Discussion started: 5 February 2020

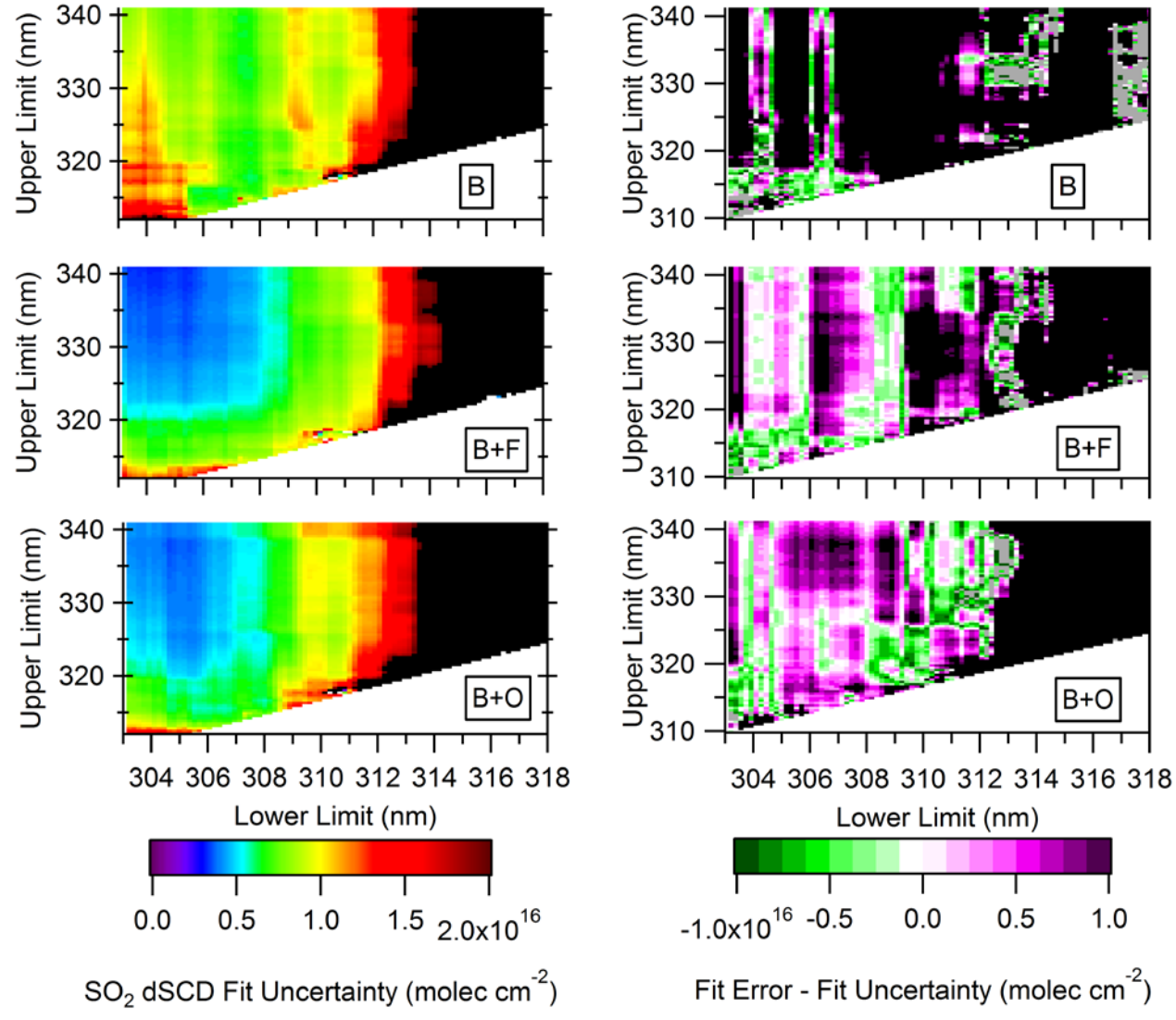

Figure 10 Low concentration SO_2 dSCDs fit errors (left) and difference between fit uncertainty and error (right) from spectra measured at 2° elevation angle for the base case (B), with offset (B+O), and with filter (B+F). Black areas indicate errors of $>2.2\times10^{16}$ molec cm^{-2} for absolute error (left) and $>1.1\times10^{16}$ molec cm^{-2} under-estimation of the fit error by the fit uncertainty.

https://doi.org/10.5194/amt-2019-420
Preprint. Discussion started: 5 February 2020

Atmospheric Measurement Techniques Discussions

References

Bobrowski, N. and Platt, U.: SO2/BrO ratios studied in five volcanic plumes, J. Volcanol. Geotherm. Res., 166(3–4), 147–160, doi:10.1016/j.jvolgeores.2007.07.003, 2007.

Bobrowski, N., Kern, C., Platt, U., Hoermann, C. and Wagner, T.: Novel SO2 spectral evaluation scheme using the 360-390 nm wavelength range, Atmospheric Meas. Tech., 3(4), 879–891, doi:10.5194/amt-3-879-2010, 2010.

Bogumil, K., Orphal, J., Homann, T., Voigt, S., Spietz, P., Fleischmann, O. C., Vogel, A., Hartmann, M., Kromminga, H., Bovensmann, H., Frerick, J. and Burrows, J. P.: Measurements of molecular absorption spectra with the SCIAMACHY pre-flight model: instrument characterization and reference data for atmospheric remote-sensing in the 230–2380 nm region, J. Photochem. Photobiol. Chem., 157(2–3), 167–184, doi:10.1016/S1010-6030(03)00062-5, 2003.

Choudhury, A. K. R., Prayagi, K. P., Engineering Pro - York University, Skillsoft Books - York University and Textile Institute (Manchester, England): Principles of colour appearance and measurement. Volume 2: Visual measurement of colour, colour comparison and management, Woodhead Publishing Limited in association with The Textile Institute, Sawston, Cambridge, UK : [online] Available from: http://ezproxy.library.yorku.ca/login?url=http://ezproxy.library.yorku.ca/sso/skillport?context=78779 (Accessed 20 August 2019), 2015.

ECCC: NPRI Data Search - Facility and Substance Information - NOVA Chemicals (Canada) Ltd. - Corunna Site 2017, [online] Available from: https://pollution-waste.canada.ca/national-release-inventory/archives/index.cfm?do=facility_substance_summary&lang=en&opt_npri_id=0000001776&opt_report_year=2017 (Accessed 17 September 2018), 2018.

Fickel, M. and Delgado Granados, H.: On the use of different spectral windows in DOAS evaluations: Effects on the estimation of SO2 emission rate and mixing ratios during strong emission of Popocatepetl volcano, Chem. Geol., 462, 67–73, doi:10.1016/j.chemgeo.2017.05.001, 2017.

Fioletov, V. E., McLinden, C. A., Cede, A., Davies, J., Mihele, C., Netcheva, S., Li, S.-M. and O'Brien, J.: Sulfur dioxide (SO2) vertical column density measurements by Pandora spectrometer over the Canadian oil sands, Atmospheric Meas. Tech., 9(7), 2961–2976, doi:10.5194/amt-9-2961-2016, 2016.

Hermans, C., Vandaele, A. C. and Fally, S.: Fourier transform measurements of SO2 absorption cross sections:: I. Temperature dependence in the 24000–29000cm−1 (345–420nm) region, J. Quant. Spectrosc. Radiat. Transf., 110(9–10), 756–765, doi:10.1016/j.jqsrt.2009.01.031, 2009.

Honninger, G., von Friedeburg, C. and Platt, U.: Multi axis differential optical absorption spectroscopy (MAX-DOAS), Atmospheric Chem. Phys., 4, 231–254, 2004.

Institute of Environmental Physics, Heidelberg University: DOASIS - DOAS Intelligent System - Home, DOASIS [online] Available from: https://doasis.iup.uni-heidelberg.de/bugtracker/projects/doasis/ (Accessed 13 September 2019), 2009.

Irie, H., Takashima, H., Kanaya, Y., Boersma, K. F., Gast, L., Wittrock, F., Brunner, D., Zhou, Y. and Van Roozendael, M.: Eight-component retrievals from ground-based MAX-DOAS observations, Atmospheric Meas. Tech., 4(6), 1027–1044, doi:10.5194/amt-4-1027-2011, 2011.

Jin, J., Ma, J., Lin, W., Zhao, H., Shaiganfar, R., Beirle, S. and Wagner, T.: MAX-DOAS measurements and satellite validation of tropospheric NO2 and SO2 vertical column densities at a rural site of North China, Atmos. Environ., 133, 12–25, doi:10.1016/j.atmosenv.2016.03.031, 2016.

Keller-Rudek, H., Moortgat, G. K., Sander, R. and Sörensen, R.: The MPI-Mainz UV/VIS Spectral Atlas of Gaseous Molecules of Atmospheric Interest, Earth Syst. Sci. Data, 5(2), 365–373, doi:10.5194/essd-5-365-2013, 2013.

Kraus, S. G.: DOASIS A Framework Design for DOAS, Mannheim University, Mannheim, Germany. [online] Available from: https://pdfs.semanticscholar.org/c091/cbb709447d3b5b778e7bf4aff9d6a2e25861.pdf, 2006.

Kreuter, A. and Blumthaler, M.: Stray light correction for solar measurements using array spectrometers, Rev. Sci. Instrum., 80(9), 096108, doi:10.1063/1.3233897, 2009.

Kristensson, E., Bood, J., Alden, M., Nordstrom, E., Zhu, J., Huldt, S., Bengtsson, P.-E., Nilsson, H., Berrocal, E. and Ehn, A.: Stray light suppression in spectroscopy using periodic shadowing, Opt. Express, 22(7), 7711–7721, doi:10.1364/OE.22.007711, 2014.

Lindon, J. C., Tranter, G. E. and Koppenaal, D. W.: Encyclopedia of Spectroscopy and Spectrometry, 2nd ed., Elsevier, Oxford; Sand Diego, CA., 2000.

Marquard, L. C., Wagner, T. and Platt, U.: Improved air mass factor concepts for scattered radiation differential optical absorption spectroscopy of atmospheric species, J. Geophys. Res.-Atmospheres, 105(D1), 1315–1327, doi:10.1029/1999JD900340, 2000.

Noxon, J. F.: Nitrogen Dioxide in the Stratosphere and Troposphere Measured by Ground-Based Absorption Spectroscopy, Science, 189(4202), 547–549, doi:10.1126/science.189.4202.547, 1975.

Ontario Ministry of the Environment: Toronto North: Hourly Sulphur Dioxide Concentrations 34021, Air Qual. Ont. [online] Available from: http://www.airqualityontario.com/history/pollutant.php?stationid=34021&pol_code=9 (Accessed 13 September 2019), 2019.

Perner, D., Ehhalt, D., Pätz, H., Platt, U., Röth, E.-P. and Volz-Thomas, A.: OH - Radicals in the lower troposphere, Geophys. Res. Lett. - GEOPHYS RES LETT, 3, 466–468, doi:10.1029/GL003i008p00466, 1976.

Platt, U. and Stutz, J.: Differential optical absorption spectroscopy : principles and applications, Springer Verlag, Berlin., 2008.

Platt, U., Perner, D. and Patz, H.: Simultaneous Measurement of Atmospheric CH2O, O3, and NO2 by Differential Optical-Absorption, J. Geophys. Res.-Oceans Atmospheres, 84(NC10), 6329–6335, doi:10.1029/JC084iC10p06329, 1979.

Platt, U., Stutz, J., Springer E-books - York University and SpringerLink (Online service): Differential optical absorption spectroscopy: principles and applications, Springer Verlag, Berlin. [online] Available from: http://www.library.yorku.ca/eresolver/?id=1261530, 2008.

Pukite, J., Kuehl, S., Deutschmann, T., Platt, U. and Wagner, T.: Extending differential optical absorption spectroscopy for limb measurements in the UV, Atmospheric Meas. Tech., 3(3), 631–653, doi:10.5194/amt-3-631-2010, 2010.

Rix, M., Valks, P., Hao, N., Loyola, D., Schlager, H., Huntrieser, H., Flemming, J., Koehler, U., Schumann, U. and Inness, A.: Volcanic SO2, BrO and plume height estimations using GOME-2 satellite measurements during the eruption of Eyjafjallajökull in May 2010, J. Geophys. Res. Atmospheres, 117(D20), doi:10.1029/2011JD016718, 2012.

Salerno, G. G., Burton, M. R., Oppenheimer, C., Caltabiano, T., Tsanev, V. I. and Bruno, N.: Novel retrieval of volcanic SO2 abundance from ultraviolet spectra, J. Volcanol. Geotherm. Res., 181(1–2), 141–153, doi:10.1016/j.jvolgeores.2009.01.009, 2009.

Schreier, S. F., Peters, E., Richter, A., Lampel, J., Wittrock, F. and Burrows, J. P.: Ship-based MAX-DOAS measurements of tropospheric NO2 and SO2 in the South China and Sulu Sea, Atmos. Environ., 102, 331–343, doi:10.1016/j.atmosenv.2014.12.015, 2015.

Tan, W., Liu, C., Wang, S., Xing, C., Su, W., Zhang, C., Xia, C., Liu, H., Cai, Z. and Liu, J.: Tropospheric NO2, SO2, and HCHO over the East China Sea, using ship-based MAX-DOAS observations and comparison with OMI and OMPS satellite data, Atmospheric Chem. Phys., 18(20), 15387–15402, doi:10.5194/acp-18-15387-2018, 2018.

Vogel, L., Sihler, H., Lampel, J., Wagner, T. and Platt, U.: Retrieval interval mapping: a tool to visualize the impact of the spectral retrieval range on differential optical absorption spectroscopy evaluations, Atmospheric Meas. Tech., 6(2), 275–299, doi:10.5194/amt-6-275-2013, 2013.

Wang, Y., Lampel, J., Xie, P., Beirle, S., Li, A., Wu, D. and Wagner, T.: Ground-based MAX-DOAS observations of tropospheric aerosols, NO_2, SO_2 and HCHO in Wuxi, China, from 2011 to 2014, Atmospheric Chem. Phys., 17(3), 2189–2215, doi:10.5194/acp-17-2189-2017, 2017.

Xie, C., Hu, X., Zhou, L., Xie, D. and Guo, H.: Ab initio determination of potential energy surfaces for the first two UV absorption bands of SO2, J. Chem. Phys., 139(1), 014305, doi:10.1063/1.4811840, 2013.

Yang, K., Krotkov, N. A., Krueger, A. J., Carn, S. A., Bhartia, P. K. and Levelt, P. F.: Retrieval of large volcanic SO2 columns from the Aura Ozone Monitoring Instrument: Comparison and limitations, J. Geophys. Res.-Atmospheres, 112(D24), D24S43, doi:10.1029/2007JD008825, 2007.